Mast cell degranulation and calcium influx are inhibited by an *Echinacea purpurea* extract and the alkylamide dodeca-2E,4E-dienoic acid isobutylamide

By: Travis V. Gulledge, Nicholas M. Collette, Emily Mackey, Stephanie E. Johnstone, Yasamin Moazami, Daniel A. Todd, Adam J. Moeser, Joshua G. Pierce, Nadja B. Cech, and Scott M. Laster

Gulledge, Travis V.; Collette, Nicholas M.; Mackey, Emily; Johnstone, Stephanie E.; Moazami, Yasamin; Todd, Daniel A.; Moeser, Adam J.; Pierce, Joshua G.; Cech, Nadja B.; Laster, Scott M. (2018). Mast cell degranulation and calcium influx are inhibited by an Echinacea purpurea extract and the alkylamide dodeca-2E,4E-dienoic acid isobutylamide. *Journal of Ethnopharmacology 212*, 166-174. https://doi.org/10.1016/j.jep.2017.10.012

Abstract:

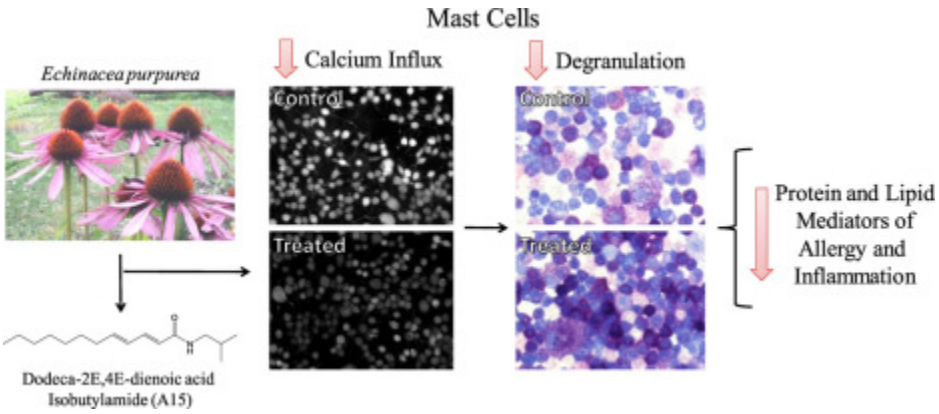

Ethnopharmacological relevance: Native Americans used plants from the genus *Echinacea* to treat a variety of different inflammatory conditions including swollen gums, sore throats, skin inflammation, and gastrointestinal disorders. Today, various *Echinacea spp*. preparations are used primarily to treat upper respiratory infections. **Aim of the study:** The goal of this study was to evaluate the effects of an ethanolic *E. purpurea* (L) Moench root extract and the alkylamide dodeca-2E,4E-dienoic acid isobutylamide (A15) on mast cells, which are important mediators of allergic and inflammatory responses. Inhibition of mast cell activation may help explain the traditional use of *Echinacea*. **Materials and methods:** A15 was evaluated for its effects on degranulation, calcium influx, cytokine and lipid mediator production using bone marrow derived mast cells (BMMCs) and the transformed rat basophilic leukemia mast cell line RBL-2H3. Methods included enzymatic assays, fluorimetry, ELISAs, and microscopy. A root extract of *E. purpurea,* and low and high alkylamide-containing fractions prepared from this extract, were also tested for effects on mast cell function. Finally, we tested A15 for effects on

calcium responses in RAW 264.7 macrophage and Jurkat T cell lines. **Results:** A15 inhibited ß-hexosaminidase release from BMMCs and RBL-2H3 cells after treatment with the calcium ionophore A23187 by 83.5% and 48.4% at 100 µM, respectively. Inhibition also occurred following stimulation with IgE anti-DNP/DNP-HSA. In addition, A15 inhibited 47% of histamine release from A23187-treated RBL-2H3 cells. A15 prevented the rapid rise in intracellular calcium following FcεRI crosslinking and A23187 treatment suggesting it acts on the signals controlling granule release. An *E. purpurea* root extract and a fraction with high alkylamide content derived from this extract also displayed these activities while fractions with little to no detectable amounts of alkylamide did not. A15 mediated inhibition of calcium influx was not limited to mast cells as A23187-stimulated calcium influx was blocked in both RAW 264.7 and Jurkat cell lines with 60.2% and 43.6% inhibition at 1 min post-stimulation, respectively. A15 also inhibited the release of TNF-α, and PGE_2 to a lesser degree, following A23187 stimulation indicating its broad activity on mast cell mediator production. **Conclusions:** These findings suggest that *Echinacea* extracts and alkylamides may be useful for treating allergic and inflammatory responses mediated by mast cells. More broadly, since calcium is a critical second messenger, the inhibitory effects of alkylamides on calcium uptake would be predicted to dampen a variety of pathological responses, suggesting new uses for this plant and its constituents.

Keywords: Alkylamide | *Echinacea purpurea* | Allergies | Inflammation | Mast cell

Article:

1. Introduction

Echinacea purpurea, *Echinacea angustifolia*, and *Echinacea pallida* are medicinal herbs indigenous to the United States and Canada. Native Americans used preparations of *Echinacea* roots to treat a variety of conditions associated with inflammatory and allergic disease, including swollen gums, inflamed skin, sore throats, and gastrointestinal disorders (reviewed by Kindscher (1989)). Today, various preparations of *Echinacea*, including ethanolic root extracts, capsules with ground plant material, and teas are used primarily to prevent or treat upper respiratory infections (URIs) (reviewed by Woelkart et al. (2008)).

It is currently unclear how preparations of *Echinacea* benefited Native Americans or provide relief to the people who use *Echinacea* to treat URIs. Most early studies focusing on the medicinal properties of *Echinacea* hypothesized that it provides an "immune-boost" (Rininger et al., 2000, See et al., 1997). However, as the pathological mechanisms underlying inflammatory and allergic disorders, and URIs became known (Dennis and Norris, 2015, Liu et al., 2011, Tisoncik et al., 2012, Wallace et al., 2014) it became increasingly unclear how boosting the immune system would benefit individuals already suffering from excess immune activation.

Chemical compounds studied in this article: Dodeca-2E 4E-dienoic acid isobutylamide (PubChem CID: 6443006)
Abbreviations: A15, alkylamide 15; ß-hex, beta-hexosaminidase; BMMC, bone marrow-derived mast cell; CRAC, calcium-release activated calcium; CB2, cannabinoid receptor type 2; ER, endoplasmic reticulum; FcεRI, fragment crystallizable epsilon receptor 1; IACUC, Institutional Animal Care and Use Committee; IgE, immunoglobulin E; IP3, inositol 1,4,5-trisphosphate; LPS, lipopolysaccharide; PLC-γ, phospholipase C-gamma; PGE2, prostaglandin E2; STIM-1, stromal interaction molecule 1; TNF-α, tumor necrosis factor alpha

Furthermore, much of the immunostimulatory activity in *Echinacea* extracts has been attributed to lipoproteins and lipopolysaccharides derived from either bacterial contaminants or bacterial endophytes (Pugh et al., 2008, Todd et al., 2015) and not a constitutive activity of the plant. Instead, most recent investigations of *Echinacea's* medicinal activity have focused on anti-inflammatory effects since suppression of inflammation would provide relief from many of the symptoms of the disorders listed above, including URIs. In support of this hypothesis, a number of in vitro studies have confirmed that *Echinacea* extracts can suppress production of inflammatory mediators from macrophages and T cells while suppression of inflammatory mediator production has also been demonstrated in vivo in influenza A infected mice (Fusco et al., 2010).

The inhibitory effects of *Echinacea* extracts on inflammatory mediator production with macrophages and T cells have been attributed to alkylamides (Sharma et al., 2009, Todd et al., 2015, Woelkart and Bauer, 2007). Alkylamides, also known as alkamides, are a class of fatty acid-like molecules produced by a number of medicinal plants including *Echinacea* spp., *Acmella oleracea*, and *Zanthoxylum* americanum ((Bauer et al., 1988; Hou et al., 2010; Leyte-Lugo et al., 2015) and reviewed by Boonen et al. (2012)). Each alkylamide contains an amide group, an alkyl chain, and a functional group such as isobutyl, benzyl, or methyl group. The number of carbons in the alkyl chain can vary, as well as the number and position of double and triple bonds. Alkylamide structures can be further diversified with modifications including hydroxylations and methylations (Leyte-Lugo et al., 2015). The alkylamide dodeca-2E,4E-dienoic acid isobutylamide, whose activity was examined in this report, is referred to as alkylamide 15 (A15) according to a numbering system reported previously (Cech et al., 2006). The complete relationship between alkylamide structure and function is not known. Certain alkylamides have been shown to bind the cannabinoid receptor type 2, and thereby modulate constitutive cytokine expression with human whole blood (Raduner et al., 2006), while structure-activity relationship studies have shown that the length of the alkyl chain is important for alkylamide-mediated suppression of TNF-α production from macrophages (Moazami et al., 2015).

Another key immune cell involved in allergic and inflammatory responses, is the mast cell (Graham et al., 2013, Liu et al., 2011, Wernersson and Pejler, 2014). The effects of *Echinacea* preparations, or of specific alkylamides, on mast cell responses have not been examined. Mast cells, found in mucosal and serosal tissues, contain large, dense granules filled with pre-formed inflammatory mediators. Mast cells can be activated by Ag-specific IgE loaded into FcεR1 receptors or by several toll-like and complement receptors (Gilfillan and Tkaczyk, 2006, Rivera et al., 2008, Siraganian, 2003). Within seconds after activation, mast cells and basophils (a circulating form of the mast cell) exocytose their granules releasing histamine, cytokines, chemokines, proteases, and growth factors into the surrounding tissue. Mast cells and basophils also produce cytokines, chemokines, prostaglandins, and leukotrienes by *de novo* biosynthetic pathways (Vig et al., 2008). Several recent reports suggest that mast cells may indeed be a target for *Echinacea* preparations. For example, an *E. purpurea* aerial extract reduced several parameters of allergy in ovalbumin-sensitized guinea pigs (Šutovská et al., 2015). Similarly, an *E. purpurea* root extract was shown to modulate disease in a model of atopic eczema (Oláh et al., 2017). For the first time, in this manuscript we examine the effects of the alkylamide A15,

and an ethanolic *E. purpurea* root extract, on the degranulation of mast cells and the ability of mast cells to mediate calcium signaling.

2. Materials and methods

2.1. Reagents

Dodeca-2E,4E-dienoic acid isobutylamide (A15) was synthesized at North Carolina State University (Raleigh, NC) as described previously (Moazami et al., 2015). In brief, a two-step oxidation of the commercially available diene-containing alcohol was performed to create the carboxylic acid followed by coupling with isobutyl amine (T3P®). Flash chromatography on SiO_2 was used to purify the crude reaction mixtures and performed on a Biotage Isolera utilizing Biotage cartridges and linear gradients (Biotage AB, Uppsala, Sweden). This process provided A15 in good yield and proved identical to the natural product by ^{1}H and ^{13}C NMR analysis with a Varian Mercury-VX 300, a Varian Mercury-VX 400, or a Varian Mercury-Plus 300 instrument in $CDCl_3$. All other chemicals were purchased from either Sigma-Aldrich (St. Louis, MO) or Thermo Fisher Scientific (Waltham, MA).

2.2. Mice

Male and female C57BL/6 mice (The Jackson Laboratory, Bar Harbor, ME) were housed at the Biological Resources Facility at North Carolina State University. All experiments were approved by the Institutional Animal Care and Use Committee (IACUC) at NC State University.

2.3. Cell isolation and culture

Bone marrow cells were isolated from the femurs of 6–8 week old C57BL/6 mice and cultured in RPMI-1640 containing 10% heat-inactivated FBS, 1X non-essential amino acids, 10 mM HEPES buffer, 1 mM sodium pyruvate, 100 U/mL penicillin, 100 µg/mL streptomycin, 5 ng/mL mIL-3, and 5 ng/mL mSCF for 4–6 weeks until mature, bone marrow-derived mast cells (BMMCs) were obtained, as described previously (Kuehn et al., 2010). Differentiation into >98% mast cells was confirmed through toluidine blue staining (1%, pH 1). RBL-2H3, RAW 264.7, and Jurkat cells were obtained from the American Type Culture Collection (Manassas, VA). RBL-2H3 cells were cultured in MEM supplemented with 15% heat inactivated FBS, 1X non-essential amino acids (Sigma-Aldrich), and 1 mM sodium pyruvate (Sigma-Aldrich). RAW 264.7 and Jurkat cells were cultured in DMEM supplemented with 10% FBS. FBS was obtained from Gemini Bio-Products (Sacramento, CA). For TNF-α, prostaglandin, and histamine measurements, cells were stimulated with A23187 alone or in combination with A15 for 8 hrs or 1 h for histamine release. Supernatants were collected, centrifuged at 16,000 × g for 5 min and stored at −80 °C until analysis. TNF-α sandwich ELISA kits, or PGE_2 and histamine competitive direct EIA kits were purchased from eBioscience (San Diego, CA), Enzo Life Sciences (Farmingdale, NY), or Oxford Biomedical Research (Rochester Hills, MI), respectively. Optical density was determined using a Synergy HT microplate reader (BioTek Instruments, Inc, Winooski, VT). Concentrations of each analyte were interpolated from standard curves.

2.4. ß-hexosaminidase degranulation assay

RBL-2H3 cell and BMMC degranulation was measured using a ß-hexosaminidase (ß-hex) activity assay. RBL-2H3 cells were plated into 96-well flat-bottom plates at 100,000 cells/well and BMMCs were plated into 96-well v-bottom plates (to allow cells to pellet during centrifugation) at 200,000 cells/well. Cells were incubated for 4 h before media was aspirated and replaced with vehicle or media containing 1 µg/mL mouse IgE anti-DNP (SPE-7) (Sigma-Aldrich) and incubated overnight. Prior to stimulation, cells were rinsed with calcium-containing Tyrode's buffer (1.8 mM $CaCl_2$, 135 mM NaCl, 5 mM KCl, 5.6 mM glucose, 1 mM $MgCl_2$, 0.1% BSA, 20 mM HEPES, pH 7.4). All treatments were prepared in Tyrode's buffer. RBL-2H3 cells were stimulated with either A23187 (Sigma-Aldrich) or DNP-HSA (Sigma-Aldrich) alone or in combination with A15 and incubated for 1 h at 37 °C. Ethanol was used as the vehicle for A15 and the final concentration was 1% in all degranulation experiments. Wells were then aspirated, and solutions containing A23187 alone or in combination with A15 were added and incubated for 1 h at 37 °C. After the incubation, 30 µL of supernatant was collected and incubated with 10 µL of 3.4 mg/mL p-nitrophenyl N-acetyl-ß-D-glucosaminide (p-NAG) at 37 °C for 1 h to measure the amount of ß-hex released from the cells. Excess supernatant was removed and the remaining cells were lysed with 100 µL of 0.1% Triton™ X-100 in Tyrode's buffer. 30 µL of the cell lysate was incubated with 10 µL of p-NAG to determine the amount of ß-hex remaining in the cells. The reaction was stopped by adding 100 µL of 0.2 M sodium carbonate buffer. Absorbance was read at 405 nm (A_{405}) on a BioTek Synergy HT microplate reader. The percent degranulation was calculated as the A_{405} of the supernatant divided by total absorbance (A_{405} of the supernatant + A_{405} of the lysate) x 100.

2.5. LDH cytotoxicity assay

RBL-2H3 cells were seeded at 100,000 cells/well into 96-well plates and incubated overnight prior to treatment with a range of A15 concentrations or 10 µg/mL cycloheximide. Supernatants were collected after 18 h and analyzed for lactate dehydrogenase (LDH) activity using the commercially available Pierce LDH Cytotoxicity Assay Kit according to the manufacturer's instructions (Thermo Fisher Scientific). In a 96-well plate, 50 µL of supernatant were incubated for 30 min with 50 µL of reaction mixture containing a tetrazolium salt that is reduced to formazan in the presence LDH protected from light. 50 µL of stop solution were added, and the A_{490} with A_{690} subtracted to remove background absorbance on a BioTek Synergy HT microplate reader. LDH release from vehicle treated cells was used to determine spontaneous LDH release. Additionally, lysis buffer was used to determine maximum LDH release.

2.6. Calcium assay

RBL-2H3, BMMC, RAW 264.7, or Jurkat cells were plated at 100,000, 200,000, 80,000, or 125,000 cells/well, respectively, into clear-bottom, black, 96-well plates (BioExpress, Kaysville, UT) and incubated overnight with media only or media containing IgE anti-DNP. Cells were loaded with the calcium-sensitive dye fluo-4 A.M. using the Fluo-4 Direct™ Calcium Assay Kit (Thermo Fisher Scientific) according to the manufacturer's instructions by incubating at 37 °C for 30 min followed by 30 min at room temperature. Prior to stimulation, baseline fluorescent readings were measured from triplicate wells in 5 s intervals for 1 min using a BioTek Synergy HT microplate reader with 485/20 nm excitation and 528/20 nm emission filters. Cells were then

treated with either 1 μM A23187 or 50 ng/mL DNP-BSA prepared in calcium- and magnesium-containing or calcium- and magnesium-free HBSS with 20 mM HEPES, and fluorescence was measured in 10 s intervals for 2 min. The final concentration of ethanol was 0.25% in these assays. The average baseline fluorescence of each well was subtracted from the stimulated fluorescent values to calculate the change (Δ) in RFU's and graphed as shown.

2.7. Fluorescence microscopy

RBL-2H3 cells plated and loaded with fluo-4, as described above, were treated and observed with an Axioskop 2 microscope (Zeiss, Oberkochen, Germany) using a fluorescent illuminator HXP-120 light source and images were acquired at 30, 60, or 120 s after stimulation with an AxioCam MRc5 camera (Zeiss) and AxioVision software (Zeiss).

2.8. Separation and fractionation of an *Echinacea purpurea* extract

Echinacea purpurea (L) Moench roots were purchased from Pacific Botanicals (Grants Pass, OR). A voucher specimen (NCU 633811) was deposited at the North Carolina Herbarium. An ethanolic extract (EE) was prepared and fractionated as described previously (Todd et al., 2015). Briefly, roots were collected, dried, and ground mechanically with a Wiley Mill Standard Model No. 3 (Arthur H. Thomas Co., Philadelphia, PA) to mesh size 2 mm. Roots were macerated in 75% ethanol (Pharmaco-AAPER, Shelbyville, KY) for seven days. A liquid-liquid partitioning scheme was used to generate an alkylamide-containing chloroform layer (CL) (Todd et al., 2015), which was subsequently fractionated using normal-phase flash chromatography with an automated Isco CombiFlash RF system over a RediSep Rf silica gel column (Teledyne Isco, Lincoln, NE). The eluent was collected in 13 different fractions (F1-13) based on LC-UV chromatograms with Galaxie Chromatography Workstation software (version 1.9.3.2). Concentrations of the most abundant alkylamides were quantified in each sample by LC-MS with an Acquity ultra-high performance liquid chromatography (UHPLC) system (Waters Corporation, Milford, MA) coupled to a LTQ Orbitrap XL Hybrid mass spectrometer (Thermo Fisher Scientific, Waltham, MA) and used to estimate the total alkylamide content (μg/mg extract). Results for each extract or fraction were: EE = 51 ± 8.2, CL 140 ± 4.7, F2 = below limit of quantification, F6 = 310 ± 42, F8 = 0.14 ± 0.034 (Todd et al., 2015).

2.9. Statistical analysis

Significant differences between means were determined using a Student's unpaired *t*-test, a one-way ANOVA, or a repeated measures one-way ANOVA with Dunnett's post-test to compare the significance of each dose or treatment tested with the vehicle control (Lew, 2007) using GraphPad Prism version 5.0 software (GraphPad Software, La Jolla, CA). Tests used and levels of significance are indicated in individual figure legends.

3. Results

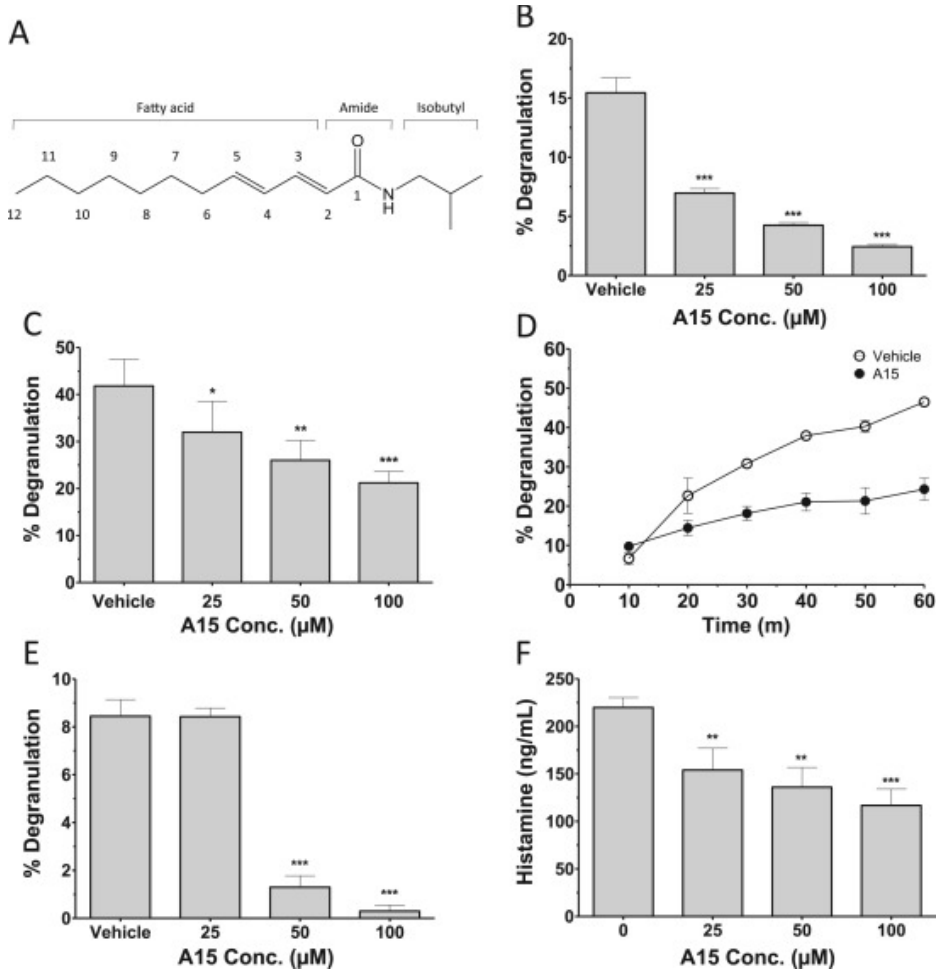

Figure 1. A15 inhibits BMMC and RBL-2H3 cell degranulation.

The structure of alkylamide A15 is shown with different functional groups and carbons in the fatty acid chain labeled (A). BMMCs were plated and stimulated 4 hrs later with 1 μM A23187 and the indicated concentrations of A15 or vehicle only. The percent degranulation was measured after 1 h (B). RBL-2H3 cells were treated with A23187 and the percent degranulation was determined 1 h later (C) or every 10 min over a 1 h time course (D). RBL-2H3 cells were plated and incubated for 4 hrs before the media was aspirated and replaced with media containing 1 μg/mL IgE anti-DNP. Cells were incubated overnight and washed prior to stimulation. The percent degranulation from RBL-2H3 cells was calculated after stimulation with 50 ng/mL DNP-HSA in combination with the indicated concentrations of A15 or vehicle only after 1 h (E). RBL-2H3 cells were stimulated for 1 h in Tyrode's buffer before supernatants were collected and levels of histamine were measured using a competitive inhibition EIA kit (F). Data shown are the means ± SEM from 3 to 4 independent experiments (B, C and F) or the means ± SEM of triplicate wells from a representative experiment from 3 independent experiments (D and E). Statistical analysis was performed using a repeated measures one-way ANOVA with Dunnett's post-hoc test, *$p<0.05$, **$p<0.01$, ***$p<0.001$.

3.1. A15 inhibits mast degranulation

In these experiments, we examined two populations of mast cells; primary bone marrow derived mast cells (BMMCs) from C57BL/6 mice, and the cell line RBL-2H3, a rat basophil-derived, transformed cell line whose degranulation pathways are similar to those of primary mast cells and basophils and frequently used to study mast cell biochemistry (reviewed by (Passante and Frankish, 2009)). With both cell types, degranulation was induced by treatment with either IgE

anti-DNP and DNP-HSA or the calcium ionophore A23187. To monitor degranulation, we measured the release of two granule components, the enzyme ß-hexosaminidase (ß-hex) and the vasoactive amine, histamine. The alkylamide we used in these studies was A15 because in experiments with monocytes and macrophages it displayed potent and broad cytokine inhibitory activity (Cech et al., 2010, Raduner et al., 2006). As shown in Fig. 1A, A15 contains an isobutyl head group, an amide group, and a 12-carbon fatty acid chain with double bonds positioned at carbons 2 and 4. Instead of isolating A15 from *E. purpurea*, A15 was chemically synthesized and analyzed by ^{1}H and ^{13}C NMR to ensure quality, as described previously (Moazami et al., 2015).

Fig. 1 panels B-F, summarize key findings for the effects of A15 on mast cell degranulation. As shown in Fig. 1B, we found that A15 inhibited the release of ß-hex from A23187-stimulated BMMCs in a dose-dependent fashion with a maximum inhibition of 83.5% ± 2.8% at a concentration of 100 μM. A15 also inhibited the release of ß-hex from A23187-stimulated RBL-2H3 cells although the level of inhibition was less than with BMMCs (48.4% ± 3.7% at 100 μM) (Fig. 1C). As shown in Fig. 1D, in experiments with A23187-treated RBL 2H3 cells, we found that inhibition of ß-hex release was apparent within 20 min after treatment began. Fig. 1E shows that A15 also inhibited degranulation from RBL-2H3 cells when they are activated by IgE anti-DNP and DNP-BSA. Finally, in Fig. 1F, we show that in addition to ß-hex, A15 also inhibited the release of the vasoactive amine histamine from RBL-2H3 cells treated with A23187 (47.0% ± 7% at 100 μM).

The data presented in Fig. 1 suggest that A15 acts biochemically to block degranulation from BMMCs and RBL-2H3 cells; however, because alkylamides have not been tested with these cells previously, we sought to reveal other explanations for these results. Lactate dehydrogenase release assays were performed to ensure that the results reported in Fig. 1 did not arise from a cytotoxic effect. As shown in Supplemental Fig. 1, we did not measure significant cytotoxic activity of A15 towards RBL-2H3 cells, even after overnight treatment, in agreement with previous studies of A15 and RAW 264.7 macrophages (Moazami et al., 2015). In addition, we tested whether A15 could inhibit the enzymatic activity of ß-hex itself. As shown in Supplemental Fig. 2, when RBL-2H3 cell lysates were incubated with the substrate (p-NAG) alone or in the presence of the indicated concentrations of A15, production of the chromogenic product was not inhibited. Finally, as shown in Fig. 2, we found that the inhibitory effects of A15 on degranulation were apparent after staining with toluidine blue. Toluidine blue is a metachromatic dye which stains nuclei blue and mast cell granules purple. Treatment of BMMCs with A23187 for 30 min noticeably reduced staining compared to control cells (Fig. 2A and C), which was blocked by A15 (Fig. 2D) confirming that A15 does indeed block release of granules from BMMCs. A15 treatment alone did not noticeably affect staining (Fig. 2B).

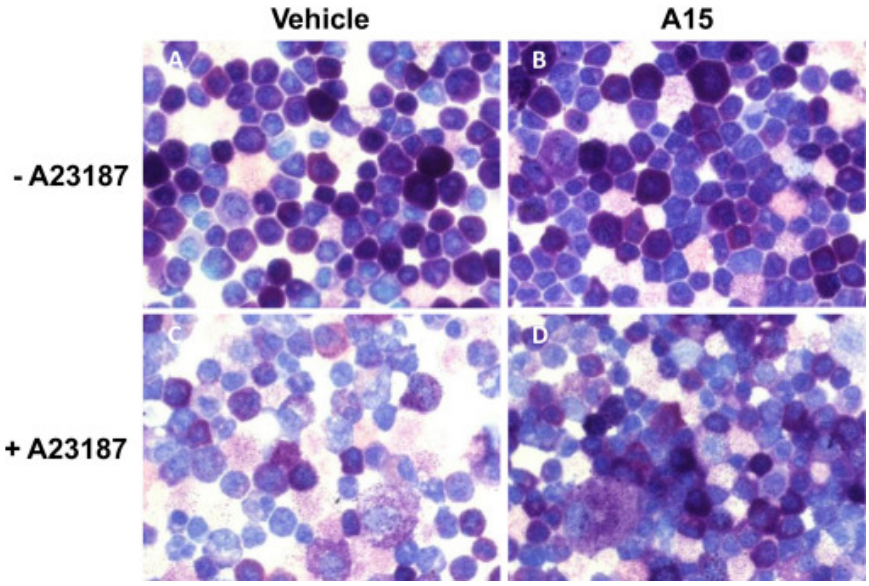

Figure 2. A15 inhibits granule release from BMMCs.
BMMCs were treated with 100 μM A15 or 0.25% ethanol only (vehicle) alone and in combination with 1 μM A23187 for 30 min. BMMCs were cytocentrifuged onto a glass slide, fixed, stained with toluidine blue (1%, pH<1) for 30 min, and washed before observing microscopically. Images were acquired at 400X magnification and are representative.

3.2. A15 blocks calcium influx in BMMCs and RBL-2H3 cells

Since A15 blocked both FcεRI and A23187-mediated degranulation, its effects likely occur via an element common to both pathways. Calcium is a key second messenger in the activation pathways of mast cells and basophils (reviewed by Gilfillan and Tkaczyk (2006)). Therefore, we hypothesized that A15 was acting to inhibit calcium mobilization in BMMCs and RBL-2H3 cells. To address this hypothesis, we utilized the calcium-sensitive fluorescent dye fluo-4 A.M. Cells were loaded with the dye, stimulated, and a multichannel absorbance plate reader was used to quantitatively examine levels of intracellular calcium. As shown in Fig. 3A, we recorded a rapid rise in levels of intracellular calcium in RBL-2H3 cells treated with A23187. The increase was noticeable after ~10 s and tended to plateau after ~60 to 80 s. We found that treatment with A15 blocked this response in a dose-dependent fashion (Fig. 3A) with 83.2% ± 5.5% inhibition measured at the 100 μM concentration of A15 (Fig. 3B). A15 also blocked the calcium response in RBL-2H3 cells treated with IgE anti-DNP and DNP-BSA (Fig. 3C and D) and in BMMCs treated with either A23187 (Fig. 3E and F) or IgE anti-DNP and DNP-BSA (Fig. 4G and H). Again, readily visible by microscopy, we found that treatment of RBL-2H3 cells with A23187 induced an increase in fluorescence, which was blocked by A15 (Supplemental Fig. 3). It should also be noted that A15 did not cause a significant change in the level of constitutive fluorescence, compared to vehicle, in unstimulated cells. For example, in Supplemental Fig. 3, analysis of pixel intensity did not reveal a significant change in fluorescence with A15 treatment ($p>0.05$, $n = 5$ fields) compared with a significant 158.4% increase with A23187 treatment ($p<0.0001$, $n=5$ fields).

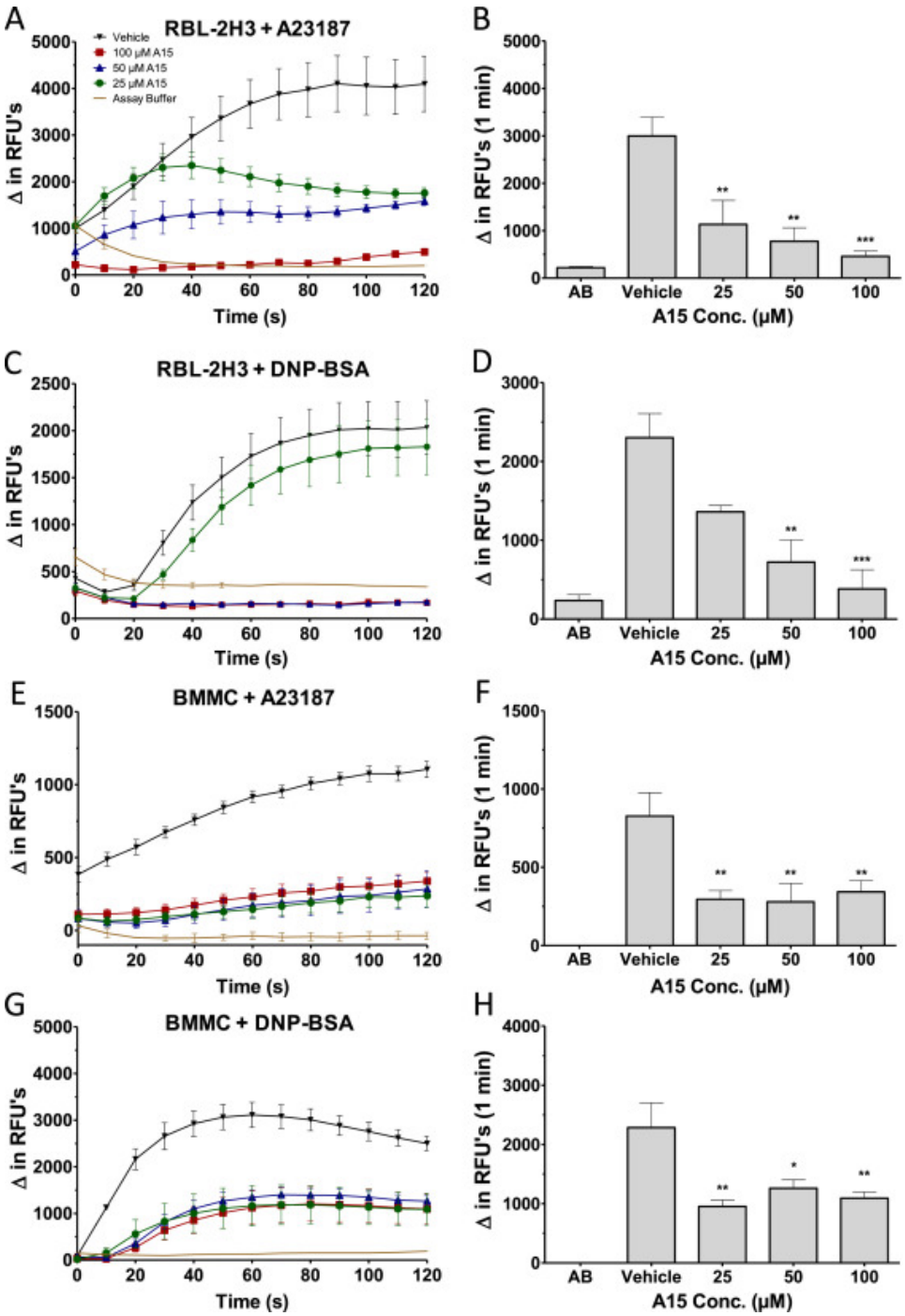

Figure 3. A15 inhibits calcium influx in RBL-2H3 cells and BMMCs.
RBL-2H3 cells (A-D) and BMMCs (E-H) were plated and incubated overnight prior to treatments. For DNP-BSA treatments, overnight incubation also included 1 µg/mL IgE anti-DNP. Prior to stimulation, cells were washed and loaded with the fluorescent, calcium-sensitive dye fluo-4 A.M. using the Fluo-4 A.M. Direct™ Calcium Assay Kit and fluorescence was measured on a microplate reader. Calcium influx was triggered in all experiments using either 1 µM A23187 or 50 ng/mL DNP-BSA, as indicated. Bar graphs represent the means ± SEM of the Δ in RFU's at 1 min post-A23187- or DNP-BSA-stimulation from 3 independent experiments (B, D, F, H). Statistical analysis was performed using a one-way ANOVA with Dunnett's post-hoc test, *p<0.05, **p<0.01, ***p<0.001.

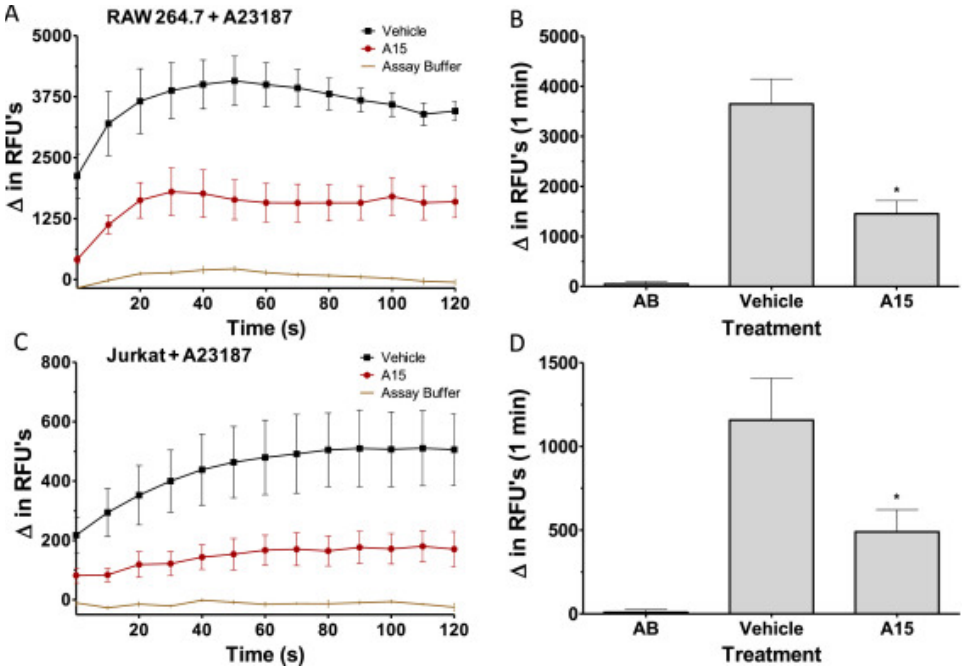

Figure 4. A15 inhibits A23187-stimulated calcium influx in RAW 264.7 and Jurkat cells. RAW 264.7 (A) or Jurkat cells (B) were loaded with fluo-4 A.M. using the Fluo-4 A.M. Direct™ Calcium Assay Kit and fluorescence was measured on a microplate reader. Cells were stimulated with 1 µM A23187 in combination with vehicle only or 100 µM A15. Bar graphs represent the means ± SEM of the Δ in RFU's at 1 min post-A23187 stimulation from 3 independent experiments. Statistical analysis was performed using an unpaired Student's *t*-test, *p<0.05.

3.3. A15 inhibits calcium influx in A23187-stimulated RAW 264.7 and Jurkat cells

Calcium influx occurs in many cell types other than mast cells via similar store-operated calcium entry-dependent mechanisms (reviewed by Feske (2009) and Vig and Kinet (2009)). To determine if the suppression by A15 was specific to mast cells or occurred with other cell types, we stimulated fluo-4 A.M.-loaded RAW 264.7 macrophage-like cells (Fig. 4A) or Jurkat T cells (Fig. 4B) with 1 µM A23187 and/or 100 µM A15. A15 treatment significantly reduced calcium influx in both RAW 264.7 and Jurkat cells at 1 min with 60.2% and 43.6% suppression, respectively, suggesting that A15 is a general inhibitor of calcium influx.

3.4. An ethanolic *E. purpurea* root extract and high-alkylamide fractions display inhibitory activities

Since *E. purpurea* is a natural source for alkylamides including A15, we hypothesized that an *E. purpurea* extract would display mast cell inhibitory activity. To test this hypothesis, we examined an extract and fractions separated from that extract, which were characterized previously for their effects on macrophage TNF-α production (Todd et al., 2015). The extract was prepared originally from *E. purpurea* roots macerated in 75% ethanol. Liquid: liquid partitioning was then used to purify a high alkylamide chloroform layer that was then separated into fractions with varying levels of alkylamides by flash chromatography over a C18 column (Fig. 5A). A total of 18 fractions were collected, 3 of which (6, 7 and 8) contained quantifiable amounts of alkylamides determined using LC-MS and the peak area of the six most abundant

alkylamide ion-chromatograms, as described in detail previously (Todd et al., 2015). The extract and fractions were then characterized for effects on LPS-stimulated production of TNF-α by RAW 264.7 macrophage-like cells (Todd et al., 2015).

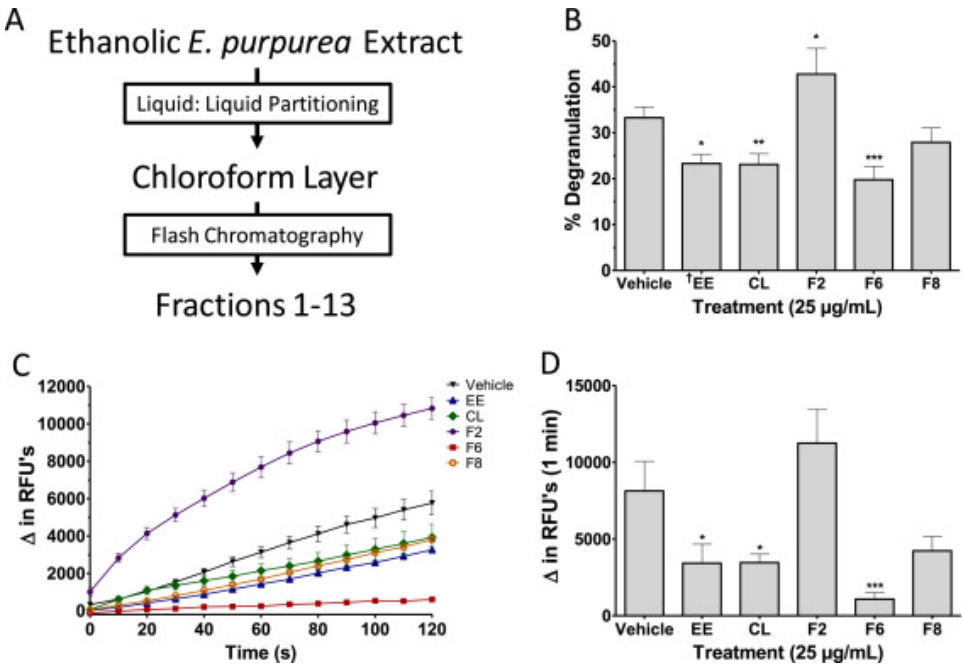

Figure 5. Alkylamide-containing *Echinacea purpurea* extracts and fractions inhibit RBL-2H3 cell degranulation and calcium influx.

A flow chart summarizing how fractions with high and low alkylamide content were prepared from an ethanolic extract of *E. purpurea* roots (A). RBL-2H3 cells were plated and incubated overnight prior to stimulation. Percent degranulation was measured 1 h after stimulation with 1 µM A23187 in combination with vehicle only or 25 µg/mL of the indicated *E. purpurea* samples. (B). RBL-2H3 cells were loaded with fluo-4 A.M. using the Fluo-4 A.M. Direct™ Calcium Assay Kit and fluorescence was measured on a microplate reader. Cells were stimulated with 1 µM A23187 in combination with the indicated *E. purpurea* samples (C and D). EE = ethanolic *E. purpurea* extract, CL = chloroform layer, F2, F6, F8 = Fraction 2, Fraction 6 and Fraction 8, respectively. Results are displayed as the means ± SEM from 3 independent experiments (B and D) or the means ± SEM of triplicate wells from a representative experiment from 3 independent experiments (C). Statistical analysis was performed using a repeated measures one-way ANOVA with Dunnett's post-hoc test, *$p<0.05$, **$p<0.01$, ***$p<0.001$. †EE was tested at 50 µg/mL.

For these experiments, we tested the extract and a subset of fractions that contained distinct alkylamide content and displayed distinct activities toward TNF-α production. As shown in Fig. 5B and C, the extract (EE, 51 ± 8.2 µg of total alkylamides/mg of plant material) did indeed inhibit both degranulation and calcium movement with A23187-treated RBL-2H3 cells. The chloroform layer (CL, 140 ± 4.7 µg of total alkylamides/mg of plant material) also displayed similar inhibitory activities (Fig. 5B and C). Fraction 6 (also with high alkylamide content, i.e. 310 ± 42 µg of total alkylamides/mg of plant material) was the only fraction tested that produced statistically significant inhibition of degranulation or calcium influx. Fraction 8, with low alkylamide content, (0.14 ± 0.034 µg of total alkylamides/mg of plant material) did not produce significant inhibition of degranulation or calcium influx (Fig. 5B). Together these results suggest that inhibition of degranulation and calcium influx in mast cells requires alkylamides, and that other compounds can impact TNF-α production by macrophages. It should be noted that a

suppressive trend was noted for calcium influx with fraction 8, suggesting that the low level of alkylamides, or perhaps other molecules, are able to weakly reduce calcium influx (Fig. 5C and D). Also, fraction 2 enhanced degranulation and calcium influx (Fig. 5B–D). Fraction 2 did not contain alkylamides detected by LC-MS, and was included as a control since it was previously found to stimulate cytokine and chemokine production from RAW 264.7 macrophages and contained LPS and potentially other pathogen-associated molecular patterns (Todd et al., 2015). These compounds appear to exert similar effects on mast cells.

3.5. A15 inhibits *de novo* production of PGE_2 and TNF-α in RBL-2H3 cells

In addition to the rapid degranulatory process, mast cells initiate synthesis of newly formed pro-inflammatory mediators, including TNF-α and PGE_2, which contribute to the long-term inflammatory responses associate with allergy (Vig et al., 2008). To test if A15 blocked these responses, RBL-2H3 cells were treated with A23187 and/or A15, overnight supernatants collected, and analyte concentration determined by ELISA. As shown in Fig. 6B, A15 produced significant, dose dependent inhibition of TNF-α at all doses tested. In contrast, production of PGE_2 was weakly inhibited and only at the 100 μM concentration of A15.

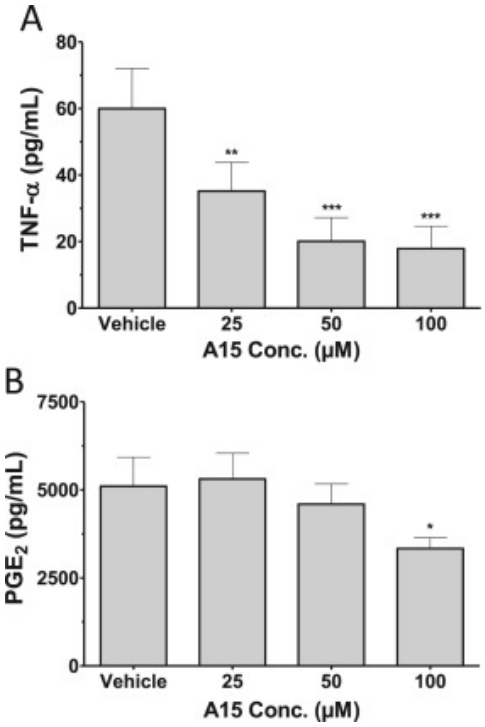

Figure 6. A15 inhibits *de novo* production of TNF-α and PGE_2 from RBL-2H3 cells.
RBL-2H3 cells were plated and incubated overnight prior to stimulation. Cells were stimulated with 1 μM A23187 in combination with the indicated doses of A15. Supernatants were collected 8 hrs later and TNF-α (A) or PGE_2 (B) levels were measured using ELISA kits. Data shown are the means ± SEM from 3 independent experiments. Statistical analysis was performed using a one-way ANOVA with Dunnett's post-hoc test, *$p<0.05$, **$p<0.01$, ***$p<0.001$.

4. Discussion

Alkylamides have been linked to the therapeutic effects of a number of medicinal plants (reviewed by Boonen et al. (2012)). Although alkylamide suppression of cytokine production has been described previously, the mechanism by which alkylamide-containing medicinal plants mediate their effects remains controversial (Boonen et al., 2012, Greger, 2016). In this report, we evaluated the effects of the alkylamide A15 on mast cell degranulation and calcium influx and found that it inhibited degranulation from RBL-2H3 cells and BMMCs (Fig. 1, Fig. 2), and this effect correlated with the suppression of calcium influx (Fig. 3). The effects of A15 on degranulation and calcium movement were not attributed to cytotoxicity (Supplemental Fig. 1). Additionally, inhibition of calcium influx was not specific to mast cells as A15 also inhibited A23187-stimulated calcium influx in RAW 264.7 macrophages and Jurkat T cells (Fig. 4). Inhibition of mast cell degranulation and calcium influx was observed by *E. purpurea* extracts and fractions with high alkylamide content, but not by fractions with little to no detectable alkylamide levels (Fig. 5). Lastly, we found that A15 inhibited *de novo* production of TNF-α and PGE_2 (Fig. 6).

In mast cells and basophils, FcεRI crosslinking leads to activation of phospholipase C-γ (PLC-γ), which causes release of endoplasmic reticulum (ER) calcium stores, followed by stromal interaction molecule-1 (STIM-1) translocation to the plasma membrane and association with Orai1, the pore-forming subunit of the calcium-release activated calcium (CRAC) channel, and influx of extracellular calcium (Baba et al., 2006, Luik et al., 2006). In contrast, ionophore treatment can transport calcium ions directly across the plasma membrane to increase calcium levels and can also cause rapid depletion of ER calcium stores and subsequent CRAC channel formation in the plasma membrane, bypassing upstream FcεRI- and PLC-γ-mediated events (Dedkova et al., 2000). A possible explanation for the effect of A15 is chelation of calcium ions to prevent influx, which would block both FcεRI- and ionophore-mediated calcium influx. However, alkylamides have not been reported to bind divalent ions previously, and known calcium chelators, such as EGTA, contain a cavity with multiple carboxyl groups to bind a calcium ion, which A15 lacks (Tsien, 1980). More likely, A15 exerts direct or indirect effects on the CRAC channel. For example, A15 could bind directly to the CRAC channel, perhaps inserting into the pore to block influx of extracellular calcium. Or, A15 could inhibit the association of STIM1 with Orai1 thereby preventing channel formation and influx of extracellular calcium. Translocation of STIM-1 to the plasma membrane occurs by movement along microtubules, and therefore, if A15 disrupts microtubule assembly, this could also explain the inhibition of calcium influx through the CRAC channel (Smyth et al., 2007). Alternatively, A15 could have a disruptive effect on membranes causing membrane-spanning ion channels (in the plasma membrane or the ER) to change conformation and prevent ion movement. Several of these hypotheses could also explain the ability of other alkylamides to inhibit the movement of potassium and sodium ions in neurons (Bautista et al., 2008, Ottea et al., 1990, Tsunozaki et al., 2013).

In these experiments we found that A15 substantially blocked production of TNF-α from RBL-2H3 cells, but its inhibitory effect on PGE_2 production was less, similar to results we found previously with RAW 264.7 macrophage-like cells (Cech et al., 2010). Production of both TNF-α and PGE_2 both likely involve calcium-dependent processes (Gronich et al., 1990, Vig et al., 2008). In mast cell types, for example, TNF-α can be released preformed from granules, which is calcium-dependent, and synthesized through a *de novo*, transcription-dependent pathway which

can involve calcium-dependent transcription factors such as nuclear factor of activated T cells (NFAT) (Klein et al., 2011). The PGE_2 pathway may also involve calcium-dependent transcription factors and calcium is also required for activation of cytosolic phospholipase A_2, the first enzyme in the biosynthetic pathway which cleaves arachidonic acid from membrane phospholipid (Gronich et al., 1990). At present, it is unclear why PGE_2 production is relatively resistant to treatment with A15. Calcium responses may recover after several hours of treatment with A15, which are sufficient to drive production of PGE_2 in overnight assays. In contrast, the production of TNF-α may be more highly dependent on the immediate calcium response which was strongly inhibited by A15. A complete analysis of the effects of A15 on these pathways will be necessary to more fully understand the effects of A15 on cytokine and lipid mediator production.

Alkylamides have been linked to the anti-inflammatory effects of *E. purpurea* and shown to inhibit cytokine, chemokine and prostaglandin production from influenza A-stimulated macrophages in vitro (Cech et al., 2010, LaLone et al., 2007). Although the role of alveolar macrophages in response to influenza infection is well-known, it was recently reported that mast cells are critical to the pathogenesis of influenza infection (Graham et al., 2013). These findings suggest that the beneficial effects of *E. purpurea* extracts for colds and flu could be due to inhibition of mast cell degranulation, a possibility that has not been explored previously. It is also possible that *E. purpurea* extracts with high alkylamide content could be useful for treating other forms of allergic inflammation mediated by mast cells such as hypersensitive reactions of the skin (Oláh et al., 2017), asthma (Šutovská et al., 2015), or allergic gastrointestinal disorders (in accord with the original use of the plant by Native Americans).

In addition to their effects on cytokine and chemokine production, alkylamides, including spilanthol and sanshool, have been linked to the tingling, analgesic activity of extracts made from alkylamide-producing plants such as *E. purpurea, A. oleracea* and *Z. americanum* (Albin and Simons, 2010, Bryant and Mezine, 1999, Ley et al., 2006). The numbing effects of alkylamides have been linked to activation of the capsaicin receptor, TRPV1 (Sugai et al., 2005). In addition, alkylamides have been shown to inhibit potassium movement through two-pore domain potassium channels (KCNK3, KCNK9, and KCNK18), which are anesthetic-targeted channels (Bautista et al., 2008, Liu et al., 2004, Talley and Bayliss, 2002). Interestingly, Bautista *et al.* found that the treatment of neurons with 100 μM sanshool caused calcium influx that was dependent on extracellular calcium (Bautista et al., 2008). In contrast, with RBL-2H3 cells or BMMCs, A15 itself did not cause a calcium response (Supplemental Fig. 3D–F) perhaps suggesting differences in the activity of A15 and sanshool, or varying effects of alkylamides on neurons versus mast cells.

In conclusion, the alkylamide A15 from *E. purpurea* inhibits mast cell degranulation and calcium influx. The beneficial effects of *E. purpurea* extracts to patients with upper respiratory tract infections may be due to the suppressive effects of alkylamides on mast cell activation. It remains to be determined if structural improvements to A15 could result in a molecule with increased activity. The combined effects of A15 on mast cell activation with previous reports of cytokine suppression from macrophages supports the use of A15 and *E. purpurea* extracts with high alkylamide content for limiting inflammation associated with infections as well as allergic responses.

Acknowledgements. We thank Dr. Susan D′Costa for her technical assistance. This work was supported by grants from the National Center for Complementary and Integrative Health, a component of the National Institutes of Health (1R15AT007259), the National Institutes of Health (R01 HD072968 to AJM), grant #54333 from the Research and Innovation Seed Fund at North Carolina State University, the Departments of Biological Sciences and Chemistry at North Carolina State University, and the Comparative Medicine Institute at North Carolina State University.

Declaration of conflicting interests. The authors declare no conflicting interests in regards to the authorship, research, and/or publication of this manuscript.

Author's contributions. TVG, NMC, EM, SEM, YM, DAT, JGP, NBC, and SML designed the experiments. TVG, NMC, YM, DAT, EM, and SEJ performed the experiments and analyzed the results. TVG and SML wrote the manuscript. TVG, NMC, AJM, JGP, NBC corrected the manuscript. All authors read and approved the final manuscript.

Appendix A. Supplementary material

Supplementary data associated with this article can be found at http://dx.doi.org/10.1016/j.jep.2017.10.012.

References

Albin, K.C., Simons, C.T., 2010. Psychophysical evaluation of a Sanshool Derivative (Alkylamide) and the elucidation of mechanisms subserving tingle. PLoS One 5 (3), e9520.

Baba, Y., Hayashi, K., Fujii, Y., Mizushima, A., Watarai, H., Wakamori, M., Numaga, T., Mori, Y., Iino, M., Hikida, M., 2006. Coupling of STIM1 to store-operated Ca2+ entry through its constitutive and inducible movement in the endoplasmic reticulum. Proc. Natl. Acad. Sci. USA 103 (45), 16704‑16709.

Bauer, R., Remiger, P., Wagner, H., 1988. Alkamides from the roots of Echinacea purpurea. Phytochemistry 27 (7), 2339‑2342.

Bautista, D.M., Sigal, Y.M., Milstein, A.D., Garrison, J.L., Zorn, J.A., Tsuruda, P.R., Nicoll, R.A., Julius, D., 2008. Pungent agents from Szechuan peppers excite sensory neurons by inhibiting two-pore potassium channels. Nat. Neurosci. 11 (7), 772‑779.

Boonen, J., Bronselaer, A., Nielandt, J., Veryser, L., De Tré, G., De Spiegeleer, B., 2012. Alkamid database: chemistry, occurrence and functionality of plant N-alkylamides. J. Ethnopharmacol. 142 (3), 563‑590.

Bryant, B.P., Mezine, I., 1999. Alkylamides that produce tingling paresthesia activate tactile and thermal trigeminal neurons. Brain Res. 842 (2), 452‑460.

Cech, N.B., Eleazer, M.S., Shoffner, L.T., Crosswhite, M.R., Davis, A.C., Mortenson, A.M., 2006. High performance liquid chromatography/electrospray ionization mass spectrometry for simultaneous analysis of alkamides and caffeic acid derivatives from Echinacea purpurea extracts. J. Chromatogr. A 1103 (2), 219‑228.

Cech, N.B., Kandhi, V., Davis, J.M., Hamilton, A., Eads, D., Laster, S.M., 2010. Echinacea and its alkylamides: effects on the influenza A-induced secretion of cytokines, chemokines, and PGE2 from RAW 264.7 macrophage-like cells. Int. Immunopharmacol. 10 (10), 1268‑1278.

Dedkova, E.N., Sigova, A.A., Zinchenko, V.P., 2000. Mechanism of action of calcium ionophores on intact cells: ionophore-resistant cells. Membr. Cell Biol. 13 (3), 357‑368.

Dennis, E.A., Norris, P.C., 2015. Eicosanoid storm in infection and inflammation. Nat. Rev. Immunol. 15 (8), 511‑523.

Feske, S., 2009. ORAI1 and STIM1 deficiency in human and mice: roles of store-operated Ca2+ entry in the immune system and beyond. Immunol. Rev. 231 (1), 189‑209.

Fusco, D., Liu, X., Savage, C., Taur, Y., Xiao, W., Kennelly, E., Yuan, J., Cassileth, B., Salvatore, M., Papanicolaou, G.A., 2010. Echinacea purpurea aerial extract alters course of influenza infection in mice. Vaccine 28 (23), 3956‑3962.

Gilfillan, A.M., Tkaczyk, C., 2006. Integrated signalling pathways for mast-cell activation. Nat. Rev. Immunol. 6 (3), 218‑230.

Graham, A.C., Hilmer, K.M., Zickovich, J.M., Obar, J.J., 2013. Inflammatory response of mast cells during influenza A virus infection is mediated by active infection and RIG-I signaling. J. Immunol. 190 (9), 4676‑4684.

Greger, H., 2016. Alkamides: a critical reconsideration of a multifunctional class of unsaturated fatty acid amides. Phytochem. Rev. 15 (5), 729‑770.

Gronich, J.H., Bonventre, J.V., Nemenoff, R.A., 1990. Purification of a high-molecular-mass form of phospholipase A2 from rat kidney activated at physiological calcium concentrations. Biochem. J. 271 (1), 37‑43.

Hou, C.C., Chen, C.H., Yang, N.S., Chen, Y.P., Lo, C.P., Wang, S.Y., Tien, Y.J., Tsai, P.W., Shyur, L.F., 2010. Comparative metabolomics approach coupled with cell-and gene-based assays for species classification and anti-inflammatory bioactivity validation of Echinacea plants. J. Nutr. Biochem. 21 (11), 1045‑1059.

Kindscher, K., 1989. Ethnobotany of purple coneflower (Echinacea angustifolia, Asteraceae) and Other Echinacea Species. Econ. Bot. 43 (4), 498‑507.

Klein, A.H., Sawyer, C.M., Zanotto, K.L., Ivanov, M.A., Cheung, S., Carstens, M.I., Furrer, S., Simons, C.T., Slack, J.P., Carstens, E., 2011. A tingling sanshool derivative excites primary sensory neurons and elicits nocifensive behavior in rats. J. Neurophysiol. 105 (4), 1701‑1710.

Kuehn, H.S., Radinger, M., Gilfillan, A.M., 2010. Measuring mast cell mediator release. Curr. Protoc. Immunol (7.38. 31-37.38. 39).

LaLone, C.A., Hammer, K.D., Wu, L., Bae, J., Leyva, N., Liu, Y., Solco, A.K., Kraus, G.A., Murphy, P.A., Wurtele, E.S., 2007. Echinacea species and alkamides inhibit prostaglandin E2 production in RAW264. 7 mouse macrophage cells. J. Agric. Food Chem. 55 (18), 7314‑7322.

Lew, M., 2007. Good statistical practice in pharmacology. Problem 2. Br. J. Pharmacol. 152 (3), 299‑303.

Ley, J.P., Krammer, G., Looft, J., Reinders, G., Bertram, H.-J., 2006. Structure-activity relationships of trigeminal effects for artificial and naturally occurring alkamides related to spilanthol. In: Wender, L.P.B., Mikael Agerlin, P. (Eds.), Developments in Food Science. Elsevier, pp. 21‑24.

Leyte-Lugo, M., Todd, D.A., Gulledge, T.V., Juzumaite, M., Carter, F.S., Laster, S.M., Cech, N.B., 2015. Cytokine-suppressive activity of a Hydroxylated alkylamide from Echinacea purpurea. Planta Med. Lett. 2 (01), e25‑e27.

Liu, C., Au, J.D., Zou, H.L., Cotten, J.F., Yost, C.S., 2004. Potent Activation of the Human Tandem Pore Domain K Channel TRESK with Clinical Concentrations of Volatile Anesthetics. Anesth. Analg. 99 (6), 1715‑1722.

Liu, F.-T., Goodarzi, H., Chen, H.-Y., 2011. IgE, Mast Cells, and Eosinophils in Atopic Dermatitis. Clin. Rev. Allergy Immunol. 41 (3), 298‑310.

Luik, R.M., Wu, M.M., Buchanan, J., Lewis, R.S., 2006. The elementary unit of store-operated Ca2+ entry: local activation of CRAC channels by STIM1 at ER‑plasma membrane junctions. J. Cell Biol. 174 (6), 815‑825.

Moazami, Y., Gulledge, T.V., Laster, S.M., Pierce, J.G., 2015. Synthesis and biological evaluation of a series of fatty acid amides from Echinacea. Bioorg. Med. Chem. Lett. 25 (16), 3091‑3094.

Oláh, Z., Rédei, D., Pecze, L., Vizler, C., Jósvay, K., Forgó, P., Winter, Z., Dombi, G., Szakonyi, G., Hohmann, J., 2017. Pellitorine, an extract of Tetradium daniellii, is an antagonist of the ion channel TRPV1. Phytomedicine 34, 44‑49.

Ottea, J.A., Payne, G.T., Soderlund, D.M., 1990. Action of insecticidal N-alkylamides at site 2 of the voltage-sensitive sodium channel. J. Agric. Food Chem. 38 (8), 1724‑1728.

Passante, E., Frankish, N., 2009. The RBL-2H3 cell line: its provenance and suitability as a model for the mast cell. Inflamm. Res. 58 (11), 737–745.

Pugh, N.D., Tamta, H., Balachandran, P., Wu, X., Howell, J.L., Dayan, F.E., Pasco, D.S., 2008. The majority of in vitro macrophage activation exhibited by extracts of some immune enhancing botanicals is due to bacterial lipoproteins and lipopolysaccharides. Int. Immunopharmacol. 8 (7), 1023–1032.

Raduner, S., Majewska, A., Chen, J.Z., Xie, X.Q., Hamon, J., Faller, B., Altmann, K.H., Gertsch, J., 2006. Alkylamides from Echinacea are a new class of cannabinomimetics Cannabinoid type 2 receptor-dependent and-independent immunomodulatory effects. J. Biol. Chem. 281 (20), 14192–14206.

Rininger, J.A., Kickner, S., Chigurupati, P., McLean, A., Franck, Z., 2000. Immunopharmacological activity of Echinacea preparations following simulated digestion on murine macrophages and human peripheral blood mononuclear cells. J. Leukoc. Biol. 68 (4), 503–510.

Rivera, J., Fierro, N.A., Olivera, A., Suzuki, R., 2008. New Insights on Mast Cell Activation via the High Affinity Receptor for IgE1, Adv. Immunol. Academic Press, pp. 85–120.

See, D.M., Broumand, N., Sahl, L., Tilles, J.G., 1997. In vitro effects of echinacea and ginseng on natural killer and antibody-dependent cell cytotoxicity in healthy subjects and chronic fatigue syndrome or acquired immunodeficiency syndrome patients. Immunopharmacology 35 (3), 229–235.

Sharma, M., Anderson, S.A., Schoop, R., Hudson, J.B., 2009. Induction of multiple proinflammatory cytokines by respiratory viruses and reversal by standardized Echinacea, a potent antiviral herbal extract. Antivir. Res. 83 (2), 165–170.

Siraganian, R.P., 2003. Mast cell signal transduction from the high-affinity IgE receptor. Curr. Opin. Immunol. 15 (6), 639–646.

Smyth, J.T., DeHaven, W.I., Bird, G.S., Putney, J.W., 2007. Role of the microtubule cytoskeleton in the function of the store-operated Ca2+ channel activator STIM1. J. Cell Sci. 120 (21), 3762–3771.

Sugai, E., Morimitsu, Y., Iwasaki, Y., Morita, A., Watanabe, T., Kubota, K., 2005. Pungent Qualities of Sanshool-Related Compounds Evaluated by a Sensory Test and Activation of Rat TRPV1. Biosci. Biotechnol. Biochem. 69 (10), 1951–1957.

Šutovská, M., Capek, P., Kazimierová, I., Pappová, L., Jošková, M., Matulová, M., Fraňová, S., Pawlaczyk, I., Gancarz, R., 2015. Echinacea complex–chemical view and anti-asthmatic profile. J. Ethnopharmacol. 175, 163–171.

Talley, E.M., Bayliss, D.A., 2002. Modulation of TASK-1 (Kcnk3) and TASK-3 (Kcnk9) Potassium Channels: volatile Anesthetics and Neurotransmitters Share a Molecular Site of Action. J. Biol. Chem. 277 (20), 17733‑17742.

Tisoncik, J.R., Korth, M.J., Simmons, C.P., Farrar, J., Martin, T.R., Katze, M.G., 2012. Into the eye of the cytokine storm. Microbiol. Mol. Biol. Rev. 76 (1), 16‑32.

Todd, D.A., Gulledge, T.V., Britton, E.R., Oberhofer, M., Leyte-Lugo, M., Moody, A.N., Shymanovich, T., Grubbs, L.F., Juzumaite, M., Graf, T.N., Oberlies, N.H., Faeth, S.H., Laster, S.M., Cech, N.B., 2015. Ethanolic Echinacea purpurea Extracts Contain a Mixture of Cytokine-Suppressive and Cytokine-Inducing Compounds, Including Some That Originate from Endophytic Bacteria. PLoS One 10 (5), e0124276.

Tsien, R.Y., 1980. New calcium indicators and buffers with high selectivity against magnesium and protons: design, synthesis, and properties of prototype structures. Biochemistry 19 (11), 2396‑2404.

Tsunozaki, M., Lennertz, R.C., Vilceanu, D., Katta, S., Stucky, C.L., Bautista, D.M., 2013. A ‘toothache tree’ alkylamide inhibits Aδ mechanonociceptors to alleviate mechanical pain. J. Physiol. 591 (13), 3325‑3340.

Vig, M., Kinet, J.-P., 2009. Calcium signaling in immune cells. Nat. Immunol. 10 (1), 21‑27.

Vig, M., DeHaven, W.I., Bird, G.S., Billingsley, J.M., Wang, H., Rao, P.E., Hutchings, A.B., Jouvin, M.-H., Putney, J.W., Kinet, J.-P., 2008. Defective mast cell effector functions in mice lacking the CRACM1 pore subunit of store-operated calcium release-activated calcium channels. Nat. Immunol. 9 (1), 89‑96.

Wallace, K.L., Zheng, L.-B., Kanazawa, Y., Shih, D.Q., 2014. Immunopathology of inflammatory bowel disease. World J. Gastroenterol. 20 (1), 6‑21.

Wernersson, S., Pejler, G., 2014. Mast cell secretory granules: armed for battle. Nat. Rev. Immunol. 14 (7), 478‑494.

Woelkart, K., Bauer, R., 2007. The Role of Alkamides as an Active Principle of Echinacea. Planta Med. 73 (07), 615‑623.

Woelkart, K., Linde, K., Bauer, R., 2008. Echinacea for Preventing and Treating the Common Cold. Planta Med. 74 (06), 633‑637.